

AN APPLICATION OF PULSED INFRARED THERMAL IMAGING IN THE DIAGNOSIS OF DIABETIC MICROANGIOPATHY

by

Yanying YIN^a, Chen LI^{a*}, and Ge SONG^b

^aDepartment of Neurology, The Fifth Central Hospital of Tianjin, Tianjin, China

^bDepartment of Clinical Medicine, Xinxiang Medical University, Henan, China

Original scientific paper

<https://doi.org/10.2298/TSCI180913213Y>

Diabetic microangiopathy is an important cause of morbidity and mortality of diabetes foot ulcers. Its early detection is very important for early intervention avoiding severe clinical symptoms. In this article, theoretical study on a pulsed infrared thermal imaging technology detecting early diabetic microangiopathy in lower extremity was carried out. The working principle of pulsed infrared thermal imaging technology was described and the 3-D thermal conduction model for atherosclerotic plaque in microvessel of distal lower extremity using pulsed infrared thermal imaging technology was established and calculated. The effect of atherosclerotic plaque geometry size including length and thickness to the measurement parameter was studied, and the influence law has been got, which can provide a theoretical basis for the diagnosis of diabetic microangiopathy using pulsed infrared thermal imaging technology.

Key words: *heat conduction, thermal imaging, geometry size, diabetic cutaneous microangiopathy*

Introduction

Diabetic microangiopathy is a major vascular complication in diabetic patients. Diabetic retinopathy, diabetic nephropathy, diabetic peripheral neuropathy, and diabetic foot ulcers are the main clinical manifestations in diabetic microangiopathy. Fundus fluorescein angiography was used to examine diabetic retinopathy, urine microprotein detection can help diagnose diabetic nephropathy, diagnosis of diabetic peripheral neuropathy is mainly based on clinical symptoms and nerve conduction measurements [1]. While diabetic foot ulcers can only be diagnosed when the clinical symptoms are obvious, which often faces the risk of amputation at the same time [2]. Studies have shown that diabetic foot ulcers was the first cause of non-traumatic amputation, with the amputation rate as high as 26.4% [3]. Now it was believed that diabetic foot ulcers was the result of many factors, including neuropathy, vascular disease, infection and so on in the distal lower extremity [4, 5]. Among them, early distal microangiopathy of lower extremity may be a major factor affecting distal peripheral neuropathy and peripheral macroangiopathy. The main characteristic of early distal microangiopathy of lower extremity is atherosclerotic changes of microangiopathy caused by basement membrane thickening and deposition of transparent substances [6]. Unfortunately, there was still a lack of method to detect atherosclerotic changes in microangiopathy. Only the presence of atherosclerotic plaques

* Corresponding author, e-mail: lichenokk@163.com

in the large vessels of the lower extremities can be detected by doppler ultrasound or CT angiography [7], however, the treatment was irreversible when macrovascular disease occurs. Therefore, early detection of lower extremity microvascular atherosclerotic lesions is helpful for early intervention, reversal of pathological changes of microvascular disease, improvement of prognosis and quality of life.

Based on the thermal effect theory of biological tissue, the researches of medical application of infrared technology and biomedical heat transfer were carried out, and formed the infrared medical thermal imaging technology (IMTIT). The IMTIT is a product of the combination of medical technology, infrared technology, and computer multimedia technology, which can record the temperature field of human body. Although current structural imaging detection (MR, CT, X-ray, and ultrasound) can provide pathological information of abnormal body structure, it cannot reflect the functional changes of body tissues. When diseases occurred, functional changes are earlier than structural changes. The dynamic observation of body function is more precursory than static observation. The technology using long-pulsed infrared thermal wave for testing breast and skin diseases was mature, and increasing studies of this technology theoretical in these disease emerged in [8, 9]. However, whether the long-pulsed infrared thermal wave testing technology can be used to detect diabetic microangiopathy was seldom studied. Only fewer clinical case-control studies occurred in this field [10]. Moreover, there was lack of relevant theoretical research of long-pulsed infrared thermal wave technology for detecting diabetic microangiopathy.

The principle of pulsed infrared thermal imaging technology

Infrared thermal imaging technology is a new non-destructive testing method developed in recent years, which has the advantages of non-contact, high efficiency, real-time, *etc.* The technology has developed rapidly and has been applied more and more widely in the field of biomedicine. Active infrared thermal imaging technology can often achieve better detection results and various external thermal excitation modes can be used. The diagnostic principle of pulse infrared thermal imaging technology is: active heating of tissue by pulse excitation source, and heat flow propagates within the tissue. Because the thermophysical parameters of lesions and non-lesions are different, the corresponding surface temperatures are different. Therefore, according to the difference of temperature distribution on the tissue surface, we can judge whether the lesion is or not and the degree of the lesion.

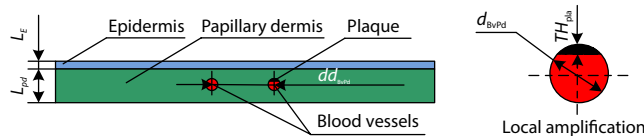


Figure 1. Structure of the geometric model

heat generation. In this section, a 3-D thermal conduction model for pulsed infrared thermal imaging in the diagnosis of diabetic microangiopathy is built. The structure size of the geometric model is shown in fig. 1 and tab. 1.

The process of the heat transfer in biological tissues can be represented [11] :

$$\rho c \frac{\partial T}{\partial t} = k \nabla^2 T + \omega_b c_b (T_a - T) + Q_m + Q(t) \quad (1)$$

The 3-D thermal conduction model

Heat transfer in biological tissues is a complicated process that involves heat conduction, blood perfusion and metabolic

where ρ is the tissue density, c – the specific heat of the tissue, T – is the local temperature of the tissue, k – the tissue thermal conductivity, ∇^2 – the second-order 3-D differential operator, ω_b – is the blood perfusion rate, c_b – is specific heat of the blood, Q_m – the metabolic heat generation rate, and $Q(t)$ – the external excitation heat source of the human skin surface, which can be written:

$$Q(t) = \begin{cases} 5 \text{ W} & 0 < t \leq 2 \text{ s} \\ 0 & t > 2 \text{ s} \end{cases} \quad (2)$$

For the skin surface, the boundary condition:

$$-k \frac{\partial T(x, y, z, t)}{\partial x} \Big|_{\text{skin surface}} = Q(t) + h_f [T_a - T(\text{skin surface}, y, z, t)] + \sigma \varepsilon [T_a^4 - T^4(H, y, z, t)] \quad (3)$$

The initial temperature is normal human body temperature, and the ambient temperature is 293.15 K. Convective heat transfer coefficient between human skin surface and surrounding air is set as 3 W/m²K. The bottom surface temperature of papillary dermis is 310.15 K. Other edge is assumed as insulated. The 3-D thermal conduction model is calculated by the COMSOL software.

Table 1. Structure size of the geometric model

Tissue layers	Epidermis	L_E [mm]	0.05, 0.10
	Papillary dermis	L_{Pd} [mm]	0.7
Blood vessels	Papillary dermis	d_{BvPd} [mm]	0.26
		dd_{BvPd} [mm]	4
Plaque		TH_{pla} [mm]	0.04, 0.06, 0.08, 0.10
		L_{pla} [mm]	2, 4, 6, 8

Results and discussions

The influence of epidermis thickness

Set papillary dermis thickness 0.7 mm, plaque thickness 0.08 mm, plaque length 4 mm, and epidermis thickness 0.05 mm and 0.1 mm, respectively. Figures 2 and 3 shows the temperature distribution on tissue surface at $t = 1.5$ s. As can be seen from the figures, the influence of epidermis thickness on the detection effect is relatively small. According to the calculation, the difference between the surface temperature of plaque corresponding tissue and

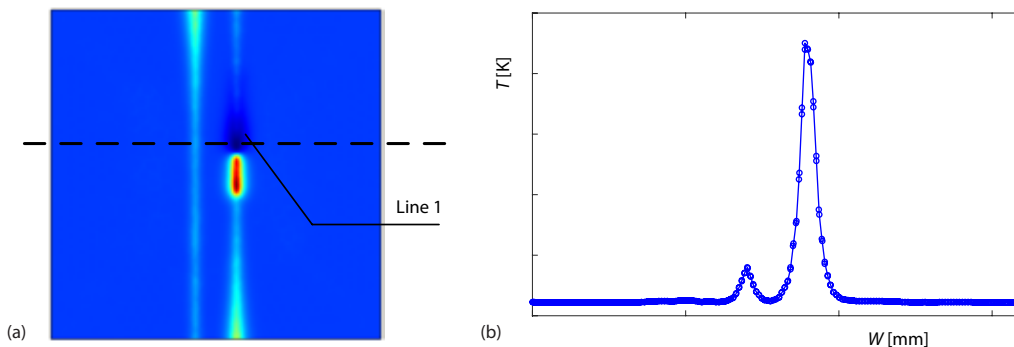


Figure 2. The temperature distribution on tissue surface at $t = 1.5$ s ($L_E = 0.05$ mm); (a) temperature distribution, Temperature distribution across the Line 1

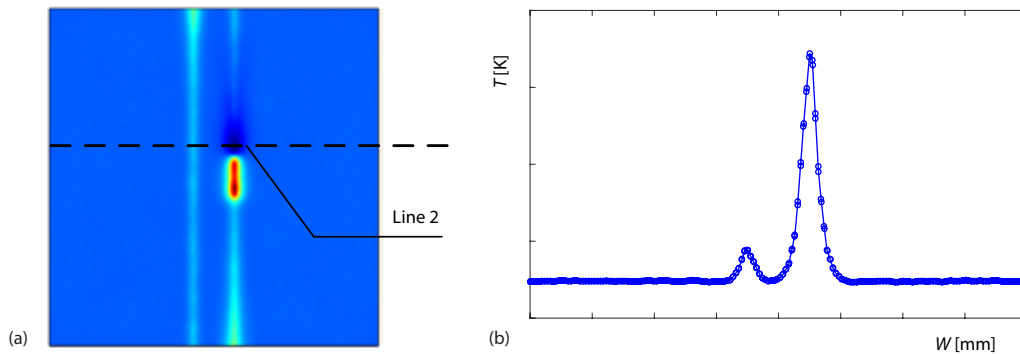


Figure 3. The temperature distribution on tissue surface at $t = 1.5$ s ($L_E = 0.10$ mm); (a) temperature distribution, (b) temperature distribution across the Line 2

that of normal tissue is about 2 K. The temperature difference of epidermis thickness 0.05 mm is slightly higher than that of 1.0 mm.

The influence of plaque thickness

Set epidermis thickness 0.1 mm, papillary dermis thickness 0.7 mm, plaque length 4 mm, and plaque thickness 0.04 mm, 0.06 mm, 0.08 mm, and 0.10 mm, respectively. Figures 4 and 5 shows the temperature distribution and difference between the surface temperature of plaque corresponding tissue and that of normal tissue according to different plaque thickness at $t = 1.5$ s. From figs. 4 and 5, it can be seen that the temperature difference increases first and then

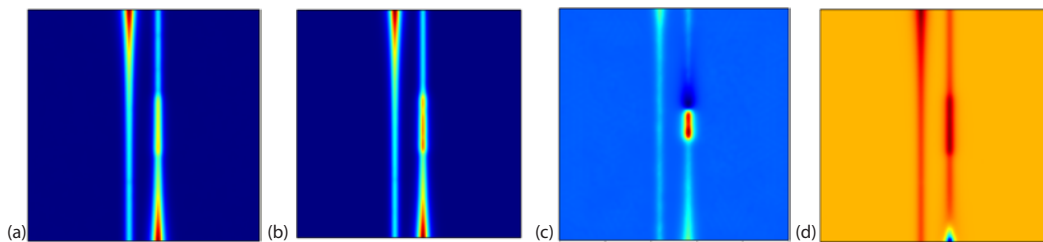


Figure 4. The temperature distribution on tissue surface vs. plaque thickness at $t = 1.5$ s ($L_{pla} = 4$ mm); (a) $TH_{pla} = 0.04$ mm, (b) $TH_{pla} = 0.06$ mm, (c) $TH_{pla} = 0.08$ mm, and (d) $TH_{pla} = 0.10$ mm

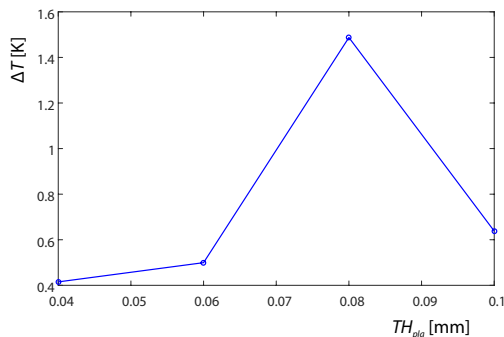


Figure 5. The temperature difference on tissue surface vs. plaque thickness at $t = 1.5$ s ($L_{pla} = 4$ mm)

decreases with the increase of plaque thickness. As the thermal conductivity of plaque is smaller than that of other normal tissues, the surface temperature difference of corresponding tissues increases with the increase of plaque thickness; on the other hand, when the plaque increases to a certain extent, the blood flow is greatly hindered and the shear viscous heat generation decreases, so the surface temperature difference begins to decrease.

The influence of plaque length

Set epidermis thickness 0.1 mm, papillary dermis thickness 0.7 mm, plaque thickness 0.08 mm, and plaque length 2 mm, 4 mm, 6 mm, and 8 mm, respectively. Figure 6 shows the temperature distribution on tissue surface at $t = 1.5$ s. Table 2 shows the temperature difference between the surface temperature of plaque corresponding tissue and that of normal tissue according to different plaque length at $t = 1.5$ s. From fig. 6 and tab. 2, it can be seen that the temperature difference decreases firstly, then increases, and then decreases with the increase of plaque length. It indicates that the effect of plaque length on the surface temperature difference of tissues is complex.

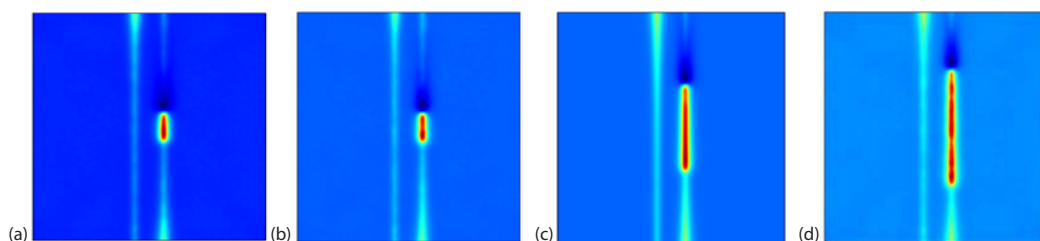


Figure 6. The temperature distribution on tissue surface vs. plaque thickness at $t = 1.5$ s ($TH_{pla} = 0.1$ mm); (a) $L_{pla} = 2$ mm (b) $L_{pla} = 4$ mm, (c) $L_{pla} = 6$ mm, and (d) $L_{pla} = 8$ mm

Conclusion

In the present study, the atherosclerotic plaques in microvessels of papillary dermis were used to simulate diabetic microangiopathy, and the plaque was modeled in 3-D. The pulsed infrared thermal imaging technology was used to detect the plaque models of different geometric sizes in the microvascular. The results showed that the epidermis temperature of the normal regions and abnormal regions in the microvascular is different. This result can be provided as the theoretical support for the clinical application.

Table 2. The temperature difference on tissue surface vs. plaque length at $t = 1.5$ s

L_{pla} [mm]	2	4	6	8
ΔT [K]	1.56	1.4873	1.5983	1.4179

Acknowledgment

The authors thank for the guidance given by endocrinologists of our hospital on diabetic small vessel disease-related knowledge, and thank Qinggong Tang engineer for the technical guidance on simulation calculation.

Nomenclature

c – specific heat, [$Jkg^{-1}K^{-1}$]
 c_b – specific heat of the blood, [$Jkg^{-1}K^{-1}$]
 k – tissue thermal conductivity, [$Wm^{-1}K^{-1}$]
 Q_m – metabolic heat generation rate, [Wm^{-3}]
 $Q(t)$ – long pulsed heat flux, [W]

Greek symbols

ρ – density, [kgm^{-3}]
 ω_b – blood perfusion rate, [s^{-1}]

References

- [1] Madonna, R., et al., Diabetic Microangiopathy: Pathogenetic Insights and Novel Therapeutic Approaches, *Vascul Pharmacol*, 90 (2017), 3, pp. 1-7
- [2] Game, F., et al., Classification of Diabetic Foot Ulcers, *Diabetes Metab Res Rev.*, 32 (2016), 1, pp. 186-94
- [3] Kim, S. Y., et al., Predictors for Amputation in Patients with Diabetic Foot Wound, *Vasc Specialist Int.*, 34 (2018), 4, pp. 109-116

- [4] Reiber, G. E., *et al.*, Causal Pathways for Incident Lower Extremity Ulcers in Patients with Diabetes from Two Settings, *Diabetes Care*, 22 (1999), 1, pp. 157-162
- [5] Jeffcoate, W. J., *et al.*, Diabetic Foot Ulcers, *Lancet*, 361 (2003), 9368, pp. 1545-1551
- [6] Volmer-Thole, M, *et al.*, Neuropathy and Diabetic Foot Syndrome, *Int J Mol Sci.*, 17 (2016), 6, pp. 917-928
- [7] Shabani Varaki, E. ,*et al.*, Peripheral Vascular Disease Assessment in the Lower Limb: A Review of Current and Emerging Non-invasive Diagnostic Methods, *Biomed Eng*, 17 (2018), 1, 61
- [8] Araujo, M. C., *et al.*, Interval Symbolic Feature Extraction for Thermography Breast Cancer Detection, *Expert Systems with Applications*, 41 (2014), 15, pp. 6728-6737
- [9] Godoy, S. E., *et al.*, Dynamic Infrared Imaging for Skin Cancer Screening, *Infrared Physics and Technology*, 70 (2015), 5, pp. 147-152
- [10] Hong, T. Z., *et al.*, Evaluation of Therapeutic Effectiveness and Prognosis in Patents with Diabetes Complicated with Lower Limb Vascular Pathological Changes by Thermal in Flared Image Technique, *Chinese Journal Clin. Rehab.*, 8 (2004), 6, pp. 1176-1177
- [11] Shih, T. C., *et al.*, Analytical Analysis of the Pennes Bioheat Transfer Equation with Sinusoidal Heat Flux Condition on Skin Surface, *Medical Engineering and Physics*, 29 (2007), 9, pp. 946-953